The formation of a systematic movement of water molecules at the vicinity of bubble in carbonated water

Shinji Karasawa. Miyagi National College of Technology, Professor emeritus.
1-3-6, Oyama, Natori-city, Miyagi-prefecture, Zip code 981-1233, Japan.
URL: http://www7b.biglobe.ne.jp/~shinji-k/index.htm
E-mail: shinji-karasawa@kbh.biglobe.ne.jp , Tel. Fax: +81-22-382-1879.

Abstract

The systematic movements of water are observed at behaviors of bubbles in carbonated water at 0℃. There exist pairing bubbles, and the sudden movement of moving bubble. The optically observable phenomena are realized by systematic movements by the condensed structure with lower energy compared with random structure of carbonated water. That is, a linear molecule of CO_2 is incorporated in the vacant 'shafts' of a helix structure (HS) of carbonated water. HS is a typical structure of tetrahedral units as that of α-quartz. The pair of hydrogen atoms in H_2O receive the force to rotate from direction of X-Y plane to direction of the 'shaft'. HS is formed as an instantaneous formation of functional structure by inter-molecular interactions. There are complex wide linkages of molecules in HS. Moreover, the systematic rotational movement exists in the HS in which the exchange of neighboring molecules occurs by thermal agitation. The systematic thermal vibration of rotations on tetrahedrons assists the transfer motion of molecules along parallel to c-axis.

The model proposed in this paper is available as a new model of liquid water for molecular dynamics, and the instantaneous formation of helix structure (HS) is available as a base of studies on the field of biochemical reactions.

1. Introduction

There are many literatures of the studies on the water [1]. The data on the structure of water were obtained by X-ray analyses, infra-red and Raman spectrums [2, 3, 4]. The properties of water have been investigated by means of molecular dynamics (MD) [5, 6. 7, 8]. The generally accepted facts are as follows. H_2O molecules in liquid or ice do not exist ionized state [9], and majority of hydrogen bonds are regarded as being in a distorted state owing to the small energy difference in the bending angle of the hydrogen bond compared with being in a broken state [10].

Water's unusual properties are concerned with systematic movement of molecules in water [11, 12], and the atomistic models of such phenomena were presented [13, 14, 15]. M. Lozynski (2015) showed a helical structure of liquid water [16]. But, following phenomena cannot explain by the traditional models. The sandwich structured bubbles in carbonated water is formed via a downsized lattice structure of water molecules. Occasional occurrences of sudden movement of bubble are realized by the formation of systematic movement of molecules.

Basing on the various properties of liquid water, the author proposes a model of dynamic state for the carbonated water. Intermolecular interactions form various intermolecular bonding structures frequently. But most of those structures will be broken by thermal movements. The helix structure (HS) of carbonated water is the condensed structure of the lower energy compared with random structure of the carbonated water. Moreover, HS possesses special movements as described later.

HS of carbonated water begins to construct from the membrane of bubble. There are similarities between HS and the structure of hexagonal ice (Ih). The inelastic neutron spectra on the ice at -3 ℃ and that of liquid water at +2 ℃ are almost identical (60~900cm^{-1}) [17]. So, a linear molecule of CO_2 in the carbonated water will be incorporated in the 'shafts' of HS. In this connection, the oxygen atom of H_2O is close to the carbon atom of CO_2 in the water-CO_2 dimer [18]. Then, the hydrogen atom of H_2O will be close to the oxygen atom of CO_2. So, the pair of hydrogen atoms of H_2O in HS rotates to the direction of paralleling to the linear molecule of CO_2. Consequently, HS is formed in the carbonated water. The proposing HS is identical to the arrangement of SiO_2 in quartz [19]. It is composed of two independent arcs made of three tetrahedral units at opposite sides of the central shaft. The transformation from α-quartz to β-quartz takes place abruptly at 573°C (846 K). The displacive phase transition from α-quartz to β-quartz results in a geometrical reduction of the size by keeping the spiral frame through a network of rotating tetrahedrons [19]. The proton-disordered structure of ice Ih is transformed into the ferroelectric ice XI at the temperature lower than 72K. The water is structurally related to the quartz because of its tetrahedral coordination.

There are the thermal motions at 0℃. The molecules in the liquid water undergo the exchange of neighboring molecules by thermal agitation. In the case where the frequency of these changes is smaller than that of the systematic rotations of tetrahedrons around the electrical axes, the systematic rotations will maintain the HS. The condensed state of trigonal symmetry of HS may include in the dynamic state of HS. It is different from vibrationally-averaged structure (V-structure).

2. Observations on the behavior of bubbles

2.1 The experimental method and experimental materials

The author tried observations on thawing ices in order to observe the systematic movements in liquid water. The photographs were taken by digital camera PENTAX Optio W 90. The close-up photos were taken in microscope mode. The frame rate of movie was a $(30)^{-1}$ second.

The materials used for the observations were prepared as follows. 100cc of tap water (Data on 50 items of impurities, ex. Pb < 0.01mg/*l*, etc. are listed at water plant of Natori city in Miyagi prefecture). Powder of dry ice (solid state of CO_2) was produced by emission from a high-pressure gas cylinder.

Materials for the observation were prepared as follows. Excess of the powder of dry ice is mixed into the water. It puts in a fridge after the white area of dry ice disappeared in carbonated water. Observations of bubbles in the carbonated water were carried out from the outside of the wide mouth

glass bottles. The bubbles exist together with ice in the carbonated water. The CO_2 molecules move through the open space in the structure of thawing ice. This is the evidence that the bubble is made of CO_2.

The clusters of water were observed at the end state of thawing ice of carbonated water. These were repeatedly generated and disappeared. The movie has been presented by S. Karasawa at website (https://youtu.be/y_jTliH36rU), (2015). In this paper, theoretical information of the liquid water is indicated by including with behaviors of bubbles in the carbonated water at 0°C.

2.2 Behaviors of bubbles in the carbonated water at 0°C.

The photographs shown in Fig.1 a), b), c), d) were captured by digital camera at 30 frames per second. The movie has been presented by S. Karasawa at website (https://youtu.be/_KRvJ5cClDk), (2016).

The rotation of bubbles inside a group along time progress is indicated in upper left side yellow circle in Fig.1.

The movement of bubbles inside of a linkage is indicated by lower red circle in Fig.1.

The whitish hazed area of water disappears at the separation of the pairing. This behavior of whitish hazed area is shown in upper right side green circle in Fig.1 a) and Fig.1 b).

a) [1/30 sec.]

b) [2/30 sec.]

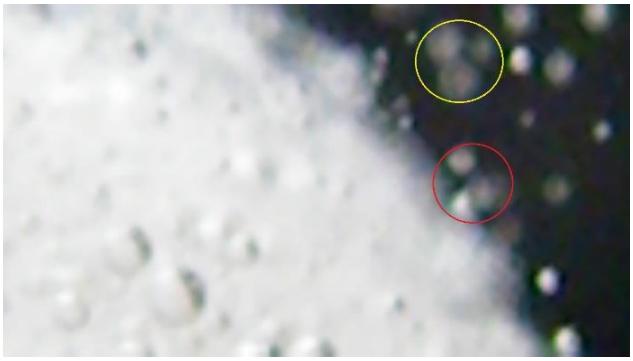

c) [3/30 sec.]

d) [4/30 sec.]

Fig.1 The whitish hazed carbonated water that is generated between pairing bubbles behaves as if it prevents from separation of carbon dioxide bubbles.

2.3 The existence of organizational structure of bubbles

Many bubbles emerged at the end of thaw of ice of carbonated water as shown in Fig.2.

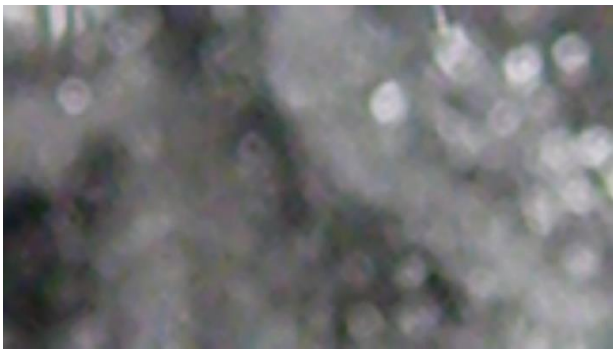

Fig.2 Many bubbles of sandwich structure are photographed at the end of thaw of ice of carbonated water.

The formation of sandwiched structure of bubbles is made by adhering of small bubbles. There are weak links between the membranes of the bubbles. The small bubbles are moving by thermal motion in a group of bubbles.

The bubble passing nearby is adhered occasionally at the torso of sandwich structure. The reaction of linkage is active

at around the torso of the sandwich structure. The connection among bubbles forms an organization of bubbles.

The moving bubble tends to induce the formation of a whitish hazed carbonated water and a sudden movement of bubble. The movement of CO_2 molecule along the open 'shaft' of HS synchronizes with the movement of H_2O molecules by the HS.

2.4 The coalescence of bubbles

A coalescence of bubbles was shown in Fig.3.a), b), c), d). These pictures were photographed by digital camera at 30 frames per second. The materials used for these observations were 100cc of carbonated water (the data were described in section 2.1) mixed with fine powder of iron (mesh #300 Fe;5g) [20]. The coalescence was observed at room temperature. These bubbles were generated in the carbonated water mixed with fine powder of iron. The period on coalescence of bubbles from beginning to end is less than 0.1 second. A sudden whitish hazed carbonated water was observed at the coalesce of bubbles as shown in Fig.3 b).

There are plural mechanisms at the coalescence of bubbles. One is the expansion of opening area at the junction of the two bubbles by the pressure of inner CO_2 gas. The other mechanism caused via the formation of HS between membranes of bubbles.

a) [1/30 sec.]

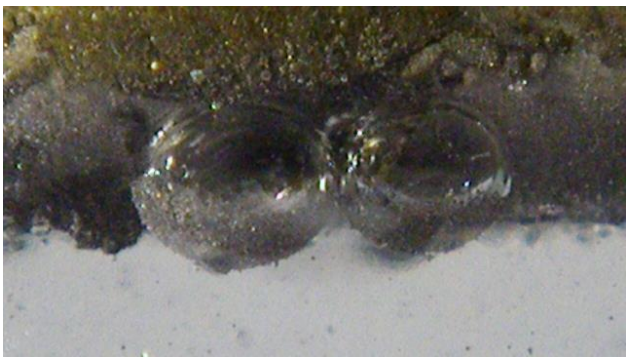

b) [2/30 sec.]

c) [3/30 sec.]

d) [4/30 sec.]

Fig.3 A coalesce of bubbles. It accompanies sudden occurrence of whitish hazed carbonated water.

3. The formation of structure of liquid water

3.1 The formation of bubbles in the carbonated water

The solubility of CO_2 in liquid water is large at the low temperature. Most of the CO_2 remains as solvated molecular CO_2. i.e. $K_h = [H_2CO_3(aq)]/[CO_{2(aq)}] = 1.7x10^{-3}$. The CO_2 is incorporated in the vacant space of the thawing state of the ice at 0℃. A bubble of CO_2 is formed through additional incorporation of CO_2 molecules. Bubbles of CO_2 are generated by the thawing state of ice because of the denser state of liquid water.

Each CO_2 has the tendency to form a linear shape owing to large size of oxygen atoms. The linear shaped molecule of CO_2 fits in the vacant shafts of HS. It promotes the formation of HS at interface of the bubble. HS bring a downsizing. The downsizing brings the lower energy state. The force of attraction between bubbles can be achieved by the formation of HS. And the whitish hazed area is explained by the formation of HS.

3.2 Instability of the regular tetrahedron in 3-dimensional structure

The low-temperature phase of ice (i.e. ice XI) possesses ferroelectricity [21, 22, 23]. And the low-temperature phase of quartz (α-quartz) possesses piezoelectricity. This fact means that, the unit of tetrahedron in 3-dimensional structure of SiO_2 or H_2O is distorted at low temperature. But the regular

tetrahedral configuration is the lowest energy state of sp^3 hybrid orbit. Also, the regular tetrahedral arrangement in the ionic bond state is the lowest energy. Moreover, the hydrogen coupling of 180 ° is the most powerful combination. These forces do not distort the ideal tetrahedron. Why does the tetrahedral unit deform?

The deformation of tetrahedral molecule was explained from the view point of "the instability of regular tetrahedral configuration" by the author as follows.

There coexist two chemical bond types of orbits in SiO_2. Those are the orbitals of covalent bond and ionic bond. The regular tetrahedron is the lowest energy lattice structure for each bonding state of orbitals. But, there are exchange interactions among coexisting orbits. The resonance structure contributes to the mutual attraction among molecules from the Valence-Bond theory [24]. The exchange energy is the maximum at the degenerate state that the energy of both electronic states become the same. The exchange energy brings an electronic degenerated state as the lower energy state at the same size of coexisting orbits. However, the degenerate state is not the lowest energy state. The lowest energy state is given by a splitting of the degenerated state. The splitting of the degenerated state is achieved by reducing of symmetry. The deformation of regular tetrahedral structure can be considered by the similar principle of the Jahn-Teller theory [25]. There is a flexibility in the degenerated electronic state. The interactions between the electronic state and the circumstance decides the deformation.

The unit of tetrahedron in 3-dimensional structure of H_2O is also distorted. But, the calculation of short-range interactions in H_2O is not easy. It requires very accurate wave functions and elaborate computational techniques, because the properties are associated with energy changes that are small compared to the total molecular energy.

3.3 Geometric contraction due to rotation of tetrahedrons in HS **-Evidence of Short-range effect-**

The network of rotation on tetrahedrons indicated in Fig.4 occurs at displacive phase transition from ß quartz to α quartz. The size of α quartz becomes small by the rotation. The change of direction on the rotation accompanies the change of polarity on the dipole moment of the tetrahedron. This phenomenon is explained at latter part of this section.

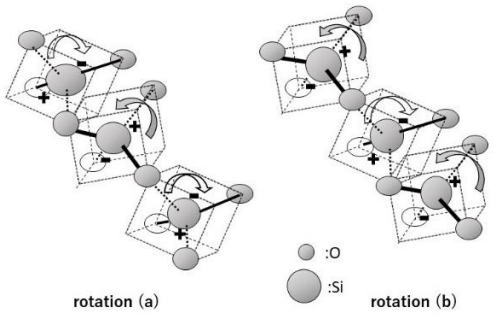

Fig.4 The change of bending angle on the points of Si-O-Si joint at α-ß displacive phase transition of the quartz. Here, small circle indicates oxygen, and thick line indicate short atomic distance. In H_2O, the polarity of polarization is reversed.

The rotation angle of ∠SiOSi can be expressed as (45°＋θ) and (45°- θ) against Z(optical) axis. The value of θ on the α-quartz is + 14 ° or -14 °. When the pressure increases, value of θ increases.

The ratio on contraction on the X-Y plane [ɤ (X, Y)] and that in the Z direction [ɤ(Z)] are given by Eq.1 and Eq.2.

$$ɤ\,(X, Y) = \frac{1+\sqrt{3}\cos(\theta)}{1+\sqrt{3}} \qquad (1).$$

$$ɤ\,(Z) = \cos(\theta) \qquad (2).$$

The axial ratio (c/a) for this geometric model of quartz (Eq.1 & Eq.2, θ=14°) is calculated as follows.

$$\frac{c(\beta)}{a(\beta)} = \frac{3}{1+\sqrt{3}} = 1.09 \qquad (3).$$

$$\frac{c(\alpha)}{a(\alpha)} = \frac{3\cos(\theta)}{1+\sqrt{3}\cos(\theta)} = 1.086 \qquad (4).$$

The axial ratio $\{c/a\}_o$ calculated from X-ray data of Bassett and Lapham[26] are given by

$$\{c_{(\beta)}/a_{(\beta)}\}_o = 1.0904 \qquad (5).$$

$$\{c_{(\alpha)}/a_{(\alpha)}\}_o = 1.0978 \qquad (6).$$

The value of axial ratio $\{c/a\}_o$ on α-quartz, i.e. Eq. (6), is larger than the other values. This observed value on α-quartz means that the X-Y plane was additionally shortened.

Interatomic distances in α-quartz were calculated by using atomic arrangement parameters (x, y, z, u). The interatomic distances listed in Table.1 were calculated by using the X-ray data of Zachariasen and Plettinger [27], Smith and Alexander [28], and Young and Post [29].

Table 1. Interatomic distances in α-quartz [Å]

	Z&P [27]	S&A [28]	Y&P [29]
$L(O_1\text{-}O_2)$	2.604	2.604	2.614
$L(O_3\text{-}O_4)$	2.632	2.639	2.640
$L(Si\text{-}O_1$ or $Si\text{-}O_2)$	1.603	1.598	1.604
$L(Si\text{-}O_3$ or $Si\text{-}O_4)$	1.616	1.616	1.611

Following relations were obtained by using data on table 1.

$$L(O_1\text{-}O_2) < L(O_3\text{-}O_4) \qquad (7).$$

$$L(Si\text{-}O_1 \text{ or } Si\text{-}O_2) < L(Si\text{-}O_3 \text{ or } Si\text{-}O_4) \qquad (8).$$

These interatomic distances indicate that each Si atom is closer to short distance side of a deformed tetrahedron in α-quartz. That is, the short distance side is the principal part of a tetrahedral unit in α-quartz. The short length side of a tetrahedron is rotated towards X-Y plane during the displacive phase transition. The long length side is rotated towards Z axis. The contraction of X-Y plane of α-quartz, that is indicated by Eq. (6), is caused by the intermolecular force of the arrangement. The

arrangement of the trigonal symmetry of HS decides the polarity of tetrahedral unit as shown in Fig.4.

The direction of rotation around X-(electric-) axis relatively easily reversed. Dauphine twins of quartz (the electric twinning) is sometimes formed by a strong vibration. The polarity of electric axes of HS is reversed on either side of the electric twinning boundary, but the optical properties are the same.

3.4 The dynamic lattice structure of liquid water

The molecule of water (H_2O) differs with the molecule of quartz (SiO_2). The direction of an electric dipole moment of H_2O unit tetrahedron opposes to SiO_2. The mobility of hydrogen atom in water is larger than that of oxygen atom in quartz. The rotational vibration of molecules in liquid water occur easily. ∠O-HO hydrogen bond angle is more easily bent than ∠HOH valence bond angle. The reorientation of electric dipole moment of water molecule due to the rotations inside of the same HS is possible to occur. This mechanism is supported by the high electric resistivity of the pure water.

L. Pauling argued that H_2O molecule units exist in the liquid state [30]. The electric dipole moment of water aligns in three directions. So, the lattice structure will be trigonal symmetry. But the crystal structure of ice Ih exhibits a hexagonal structure. It is transformed into the ferroelectric ice XI at the temperature lower than 72K. The ferroelectric state exists only under the lower temperature like a super conductive state.

The energy gap caused by the contraction due to the displacive phase transition can be roughly estimated under the following assumption. The energy gap corresponds to the change of potential energy caused by the downsize. Here, the cohesive energy of hydrogen bond is 5 kcal/mol (0.217eV). The value of down-size ratio is assumed as 0.97 [i.e. $\cos(\theta) = \cos(14^\circ) = 0.97$].

The energy gap on the displacive phase transition was estimated by using the ratio on the contraction as a rough estimation.

$$E_{gap} = 0.217[eV]x(1-0.97)=0.0065 \quad [eV] \quad (9).$$

The ice Ih is transformed into the ferroelectric ice XI at the temperature lower than $T_{transition} = 72K$ [21].

$$kT_{transition} = 72 \ [K]x8.617x10^{-5} = 0.0062 \ [eV] \quad (10).$$

The transition temperature Eq. (10) is corresponded with the energy gap of the displacive phase transition Eq. (9).

4. Linkages of water molecules in the liquid water

4.1 A model of systematic movement of water molecules

The proposing model of HS is illustrated in Fig.5 a) and b).

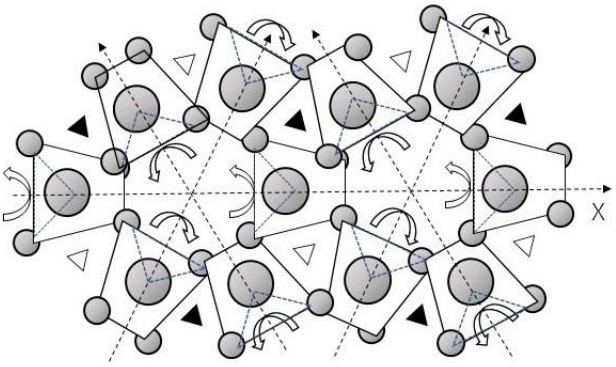

a) The angle of rotation is (45°＋θ) against Z axis.

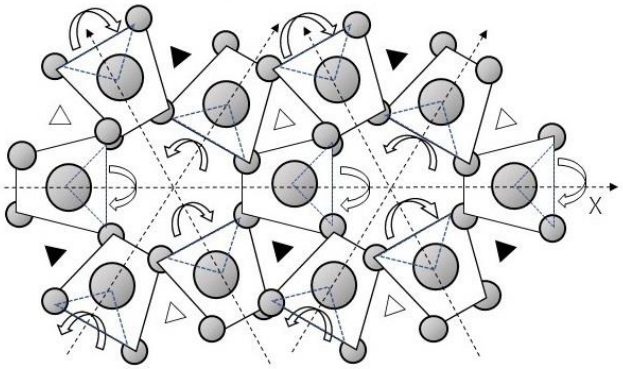

b) The angle of rotation is (45°- θ) against Z axis.

Fig.5 The linkage of water molecules at systematic rotation of tetrahedrons in HS. A trapezoid is the projected pattern onto X-Y plane on a cubic model of unit tetrahedron. A dashed triangle indicates the principal part of the unit. An oxygen atom is a large circle. A small circle is a hydrogen atom. Upward movement is △, Downward movement is ▲.

The pattern of each molecule projected on the X-Y plane is changed from a square to the trapezoid by the rotation θ. Short side of the projected trapezoid corresponds to the pair of hydrogen atoms approached to the Z axis. Long side of the trapezoid corresponds to the pair of hydrogen atoms approached to X-Y plane. A dashed triangle indicates the principal part of the tetrahedral unit. It was estimated by the similar way described in section 3.3.

4.2 Formation of HS of water molecules at a plane interface

There are the reports on nearest-neighbor oxygen-oxygen distance in ice Ih [31]. Those values are not identical. And the angles of ∠O⋯O⋯O are not exactly tetrahedral [32]. There are irregularities in the lattice structure of ice. The uncertainty about the position of hydrogen atoms is explained by the flexibility of the electronic state.

The crystal growth of ice from water was investigated by means of the molecular dynamic simulation [33, 34]. The formation of systematic structure begins at the interfaces.

The membrane of a bubble becomes the basal plane of 3-dimensional structure of water. The trigonal symmetry of the double helical structure is formed parallel to interface of the water.

Each molecule of H_2O has an electric dipole moment. The tetrahedral units are connected by the hydrogen bonds under the electric interactions among water molecules. The arrangement of short side of tetrahedron and long side are aligned as regular order along the three directions of electric axes. The pair of hydrogen atoms of each water molecule is faced to the wall of the central shaft of each HS. The H_2O in the central shaft receives the rotating force towards paralleling to c-axis via the oxygen atoms of CO_2 incorporated in the central shaft. HS is realized by the coupling between the molecule of CO_2 and hydrogen atoms of water molecule at the wall of open 'shafts' in HS. So, HS has stands along vertical direction to the X-Y plane.

4.3 A peculiar linkage of water molecules of the systematic rotation of tetrahedrons in the double helical structure

A systematic rotation of tetrahedrons easily takes place by the systematic changes of the angle on hydrogen bond in HS. The electric dipole moment of the tetrahedron will change according to the rotation of tetrahedrons around its electric axes as shown in Fig.4 (i.e. $\pm\theta$ from 45° against c-axis). This systematic thermal motion of rotating molecules of H_2O around electrical axes involves alternate change of electric potential at the wall of the open shaft as shown in Fig.5 a), b). This systematic vibration of molecules will make a swirling motion along the shaft of each spiral. It supports transportation of the molecule in the open 'shaft' of spiral structure. This mechanism is the cause of a quick movement of a bubble accompanying with the instantaneous whitening of the water around the bubbles.

4.4 The distorted hydrogen-bond model explained by model of HS

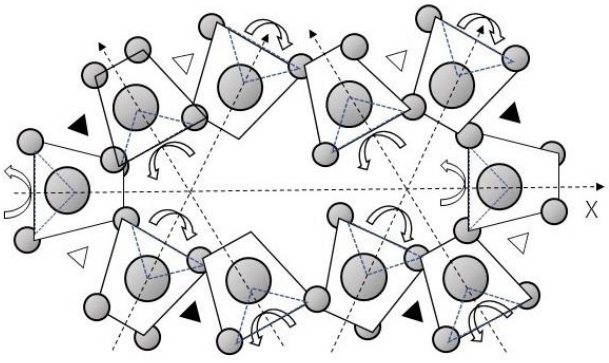

Fig.6 The imaginary state in which a vacancy of water molecule happened. A defect of molecule in HS induces various distorted HS under the constraints of the interactions among the molecules.

Fig.6 shows an illustration of the imaginary state in which a vacancy of water molecule happened. This illustration indicates large influence on the vacancy of a molecule. It means the robustness of frame of HS.

The distorted lattice structure will rearrange under constraints due to the interactions among water molecules. The area of distorted spiral structuer expands by the linkages of the lattice structure will rearrange the frame of the structure under constraints due to the interactions among water molecules. The area of distorted spiral structuer expands by the linkages of water molecules. The various deformed HS is realized at the conditions at each situation. The re-arrangement is disturbed by the thermal agitations. It is hard to attain the thermodynamic equilibrium. So, the liquid water is characterized by a wide distribution of distorted structures [10].

5. Discussions

What is the difference between HS model and Lozynski's model?

Lozynski showed that the network of tetragonal oxygen atoms in ice Ih can be converted into helical geometry [16]. It explains the phase transition between ice (Ih) and ice (XI). On the other hand, the behavior of bubbles in the carbonated water is explained by the instantaneous formation of HS. But, the snow crystal is suggesting that HS of pure water is not exist. HS is formed only under the appropriate conditions.

How does the molecular structure of liquid water extend up to macroscopic size?

The ordered structure caused by quantum mechanical interactions extends into a macroscopic size, because each unit possesses the same characteristics. There are the linkages among molecules in liquid water. The expansion of ordering brings robustness on the ordering.

Why can we observe the Brownian motion?

It is difficult to move one Brownian particle of diameter 10^{-6} m by randomized individual water molecules of diameter $3x10^{-10}$ m. Einstein's theory on Brownian motion had succeeded by avoiding of the description on individual molecule of water.

Does HS is the universal model of water?

An instantaneous structure and the averaged structure are different. HS exists under appropriate conditions at an instant. Most of data on the lattice structure of liquid water indicate disordered structures by the thermal agitations.

6. Conclusions

This paper described the systematic movements of water based on the observations of behaviors of bubbles in carbonated water at 0℃. There exist pairing bubbles, and the sudden movement of moving bubble. The optically observable phenomena are realized by systematic movements by the condensed structure with lower energy compared with random structure of carbonated water. HS is a functional structure. HS is a condensed structure with lower energy. So, HS is formed as an instantaneous formation of functional structure by inter-molecular interactions in the carbonated water. That is, a linear molecule of CO_2 is

incorporated in the vacant 'shafts' of HS in the carbonated water. The pair of hydrogen atoms of H_2O is close to the incorporated CO_2. The pair of hydrogen atoms of H_2O receives the force to change the direction towards the parallel of the central shaft. The arrangement of HS begins to grow by a cooperative phenomenon at the interface of the bubble.

The proposing model of HS is a typical structure of the carbonated water. There are complex wide linkages of molecules in HS. Moreover, the systematic rotational movement exists in the HS in which the exchange of neighboring molecules occurs by thermal agitation. The systematic thermal vibration of rotations on tetrahedrons assists the transfer motion of molecules along parallel to c-axis. It is the plausible model of functional properties of liquid water. The instantaneous formation of HS is available as a base of studies on the functional properties of the liquid water.

The author hopes that the quantitative analysis on the proposing model of liquid water will be carried out in the near future.

Acknowledgements

The author would like to thank to Professor. TAMURA, Koji, Department of Biological Science and Technology, Tokyo University of Science who gave him useful suggestions. We thank Edanz Group (www.edanzediting.com/ac) for editing draft of this manuscript.

References

1. J. L. Finney, *Phil. Trans. R. Soc. Lond.* **B 359,** 1145, (2004).
2. J. Morgan, B. E. Warren, J. Chem. Phys. **6**, 666, (1938).
3. G. E. Walrafen, J. Phys. Chem. **40**, 3249, (1964).
4. T. T. Wall, J. Chem. Phys. **51**, 1113, (1969).
5. A. Rahman, F. H. Stillinger, J. Chem. Phys. **55**. 3336, (1971).
6. H. Tanaka, I. Ohmine, J. Chem. Phys. **87**. 6128, (1987)
7. M. Cho, G. R. Fleming, S. Saito, I. Ohmine, and R. M. Strat, J. Chem. Phys. **100**, 6672 (1994).
8. J. M. Míguez, M. M. Conde, J.-P. Torré, F. J. Blas, M. M. Piñeiro, and C. Vega, J. Chem. Phys. **142,** 124505 (2015)
9. J. D. Bernal and R. H. Fowler. J. Chem. Phys. **1**, 515, (1933).
10. J. A. Pople, Proc. R. Soc. **A 205**,163, (1951).
11. S. Sastry, P. G. Debenedetti, F. Sciortino, and H. E. Stanley, Phys. Rev. **E 53**. 6144 (1996).
12. F. W. Starr, M.-C. Bellissent-Funel, and H. E. Stanley, Phys. Rev. **E 60**. 1084 (1999).
13. D. T. Limmer and D. Chandler, J. Chem. Phys. **135**, 134503 (2011).
14. K. Stokely, M. G. Mazza, H. E. Stanley, G. Franzese, Proc. Nat. Acad. Sci. USA. **107**, 1301 (2010).
15. F. Weinhold, J. Chem. Phys. **109** 373 (1998).
16. M. Lozynski, J. Chem. Phys. **455,** 1 (2015)
17. K. E. Larsson, U. Dahlborg, J. nuclear energy, Parts A/B, **16**, Issue 2, 81-89 (1962).
18. R. J. Wheatley, A. H. Harvey, J. Phys. Chem. **134**, 134309 (2011)
19. S. Karasawa, Japanese J. Applied Physics, **13**, No.5, 799, (1974).
20. S. Karasawa, Viva Origino (ISSN-0910-4003), **42**, No.3, (2014).
21. S. M. Jackson, R. W. Whitworth, J. Phys. Chem. **B 101(32)**, 6177, (1997)
22. A. J. Leadbetter, R. C. Ward, J. W, Clark, P. A. Tucker, T., Matsuo, H. Suga, J. Chem. Phys. **82,** 424, (1985).
23. H. Fukazawa, A. Hoshikawa, Y. Ishii, B. C. Chakoumakos, and J. A. Fernandez-Baca, Astrophysical Journal, **652**, L57-L60, (2006).
24. C. A. Coulson, U. Danielsson, Ark. Fys. **8**, 239, 245, (1954).
25. H. A. Jahn, E. Teller, Proc. Roy. Soc. **A161**, 220, (1937).
26. W. A. Bassett, D. M. Lapham, American Mineralogist. **42**, 548, (1957).
27. W. H. Zachariasen, H. A. Plettinger, Acta. Cryst. **18**, 710, (1965).
28. G. S. Smith, L. E. Alexander, Acta. Cryst. **16**, 462, (1963).
29. R. A. Young, B. Post, Acta. Cryst. **15**, 337, (1962).
30. L. Pauling, J. Am. Chem. Soc., **57**, 2680, (1935).
31. K. Lonsdale, Proc. R. Soc. **A 247**,424, (1958)
32. R. Brill, Angew. Chem. (Int. edit.) **1**, 563, (1962)
33. H. Nada, J. Phys. Chem. **B, 110 (33)**, 16526, (2006).
34. H. Nada, J. P. van der Eerden, Y. Furukawa, J. Crystal Growth, **266**, 297, (2004).